Carbohydrate Polymers 299 (2023) 120175

Contents lists available at ScienceDirect

Carbohydrate Polymers

journal homepage: www.elsevier.com/locate/carbpol

Structural and functional properties of alginate obtained by means of high hydrostatic pressure-assisted extraction

Hylenne Bojorges [a], Antonio Martínez-Abad [a,c], Marta Martínez-Sanz [b,c], María Dolores Rodrigo [a], Francisco Vilaplana [d], Amparo López-Rubio [a,c], María José Fabra [a,c,*]

[a] Food Safety and Preservation Department, Institute of Agrochemistry and Food Technology (IATA-CSIC), Av. Agustín Escardino 7, Paterna 46980, Valencia, Spain
[b] Instituto de Investigación en Ciencias de la Alimentación, CIAL (CSIC-UAM, CEI UAM + CSIC), Nicolás Cabrera, 9, Madrid, 28049, Spain
[c] Interdisciplinary Platform for Sustainable Plastics Towards a Circular Economy-Spanish National Research Council (SusPlast-CSIC), Madrid, Spain
[d] Division of Glycoscience, Department of Chemistry, School of Engineering Sciences in Chemistry, Biotechnology and Health, KTH Royal Institute of Technology, AlbaNova University Centre, SE-106 91 Stockholm, Sweden

ARTICLE INFO

Keywords:
HPP
Molecular weight
Nanostructure
Brown seaweed
M/G ratio
Polysaccharide extraction

ABSTRACT

The effects of the high hydrostatic pressure (HPP) pre-treatment on the alginate extraction were seen to greatly depend on the recalcitrant nature of two algae species. Alginates were deeply characterized in terms of composition, structure (HPAEC-PAD, FTIR, NMR, SEC-MALS), functional and technological properties.

The pre-treatment significantly increased the alginate yield in the less recalcitrant *A. nodosum* (AHP) also favoring the extraction of sulphated fucoidan/fucan structures and polyphenols. Although the molecular weight was significantly lower in AHP samples, neither the M/G ratio nor the M and G sequences were modified. In contrast, a lower increase in alginate extraction yield was observed for the more recalcitrant *S. latissima* after the HPP pre-treatment (SHP), but it significantly affected the M/G values of the resulting extract. The gelling properties of the alginate extracts were also explored by external gelation in $CaCl_2$ solutions. The mechanical strength and nanostructure of the hydrogel beads prepared were determined using compression tests, synchrotron small angle X-ray scattering (SAXS), and cryo-scanning electron microscopy (Cryo-SEM). Interestingly, the application of HPP significantly improved the gel strength of SHP, in agreement with the lower M/G values and the stiffer rod-like conformation obtained for these samples.

1. Introduction

Macroalgae are one of the renewable resources of the marine environment, which have received rising attention due to their important role as a valuable source of hydrocolloids and bioactive compounds (Abka Khajouei et al., 2021; Hentati et al., 2018). There are about 9000 species of macroalgae, which, depending on their photosynthetic pigments, can be classified into Chlorophyta (green), Phaeophyta (brown), and Rhodophyta (red) (Sanjeewa et al., 2018). Specifically, brown algae are rich in polysaccharides, phenolic compounds, carotenoids, proteins, vitamins, and minerals (Kadam & Prabhasankar, 2010). The main polysaccharide present in the cell wall of brown algae is alginate and can represent up to 40 % of the dry matter of the seaweed (Łabowska, Michalak, & Detyna, 2019). Alginate is a linear polymer constituted by two monomeric uronic acids, β-(1-4)-D-mannuronic acid (M block) and α-L-guluronic (G block) acid (Fertah et al., 2017). The arrangement of the monomers creates homogeneous MM, and GG blocks only composed of one uronic acid species and heterogeneous MG (or GM) blocks (Khajouei et al., 2018). The biological and physicochemical properties of alginates depend on the M/G ratio and on the structure and distribution of acid blocks in the polysaccharide backbone, which varies depending on the species, the type of tissues, age, or harvesting seasons (Karaki et al., 2013). In this regard, stiff and brittle alginate gels are known to have low M/G ratios, while elastic and flexible gels are known to have high M/G ratios. Specifically, in the food industry, they are widely used ingredients due to their stabilizing, thickening, and gelling properties (Brownlee et al., 2005), also having a role as dietary fiber. All these properties are highly affected not only by the molecular weight and M/G ratios of alginates but also by their molecular conformations (Zrid et al., 2016).

* Corresponding author at: Food Safety and Preservation Department, Institute of Agrochemistry and Food Technology (IATA-CSIC), Av. Agustín Escardino 7, Paterna, 46980, Valencia, Spain.
E-mail address: mjfabra@iata.csic.es (M.J. Fabra).

https://doi.org/10.1016/j.carbpol.2022.120175
Received 11 August 2022; Received in revised form 15 September 2022; Accepted 26 September 2022
Available online 30 September 2022

Generally, the alginate extraction process involves an acid pre-treatment to remove pigments, carbohydrates, and low molecular weight compounds. Then, an alkaline extraction is performed, followed by solid/liquid separation, drying, and milling, to produce high-quality alginate (Bojorges, Fabra, López-Rubio, & Martínez-Abad, 2022). However, some alternative and novel protocols have been proposed in the last decade (Gomez et al., 2020; Ummat, Sivagnanam, Rajauria, O'Donnell, & Tiwari, 2021; Yang et al., 2022), such as ultrasound-assisted extraction (Flórez-Fernández, Domínguez, & Torres, 2019), enzyme-assisted extraction (Borazjani, Tabarsa, You, & Rezaei, 2017), microwave-assisted extraction (Okolie, Mason, Mohan, Pitts, & Udenigwe, 2020), subcritical water extraction (Saravana, Cho, Woo, & Chun, 2018), and supercritical fluid extraction (Balboa, Moure, & Domínguez, 2015) with the aim of causing microstructural modifications in the treated seaweeds, favoring their extractability (Abka Khajouei et al., 2021). High hydrostatic pressure processing (HPP) is one of the most economically viable non-thermal treatments (Rastogi, Raghavarao, Balasubramaniam, Niranjan, & Knorr, 2010). The application of HPP is generally used to inactivate pathogens for food preservation without negatively affecting their organoleptic and functional properties (Marin et al., 2020). Likewise, it has been found that the application of HPP in extraction processes may bring about structural changes in foods, such as rupture of the plant cell walls, improving the mass transfer rate, as well as enhance the solvent permeability in plant cells and secondary metabolite diffusion (Pinton et al., 2021; Zhao, Baik, Choi, & Kim, 2014).

Recent studies have indicated that HPP may increase the extraction yield of bioactive compounds from plant sources and reduce the processing time (Malafronte et al., 2021; Schultz, Wagner, Urban, & Ulrich, 2004; Zuluaga et al., 2016). However, to the best of our knowledge, there is no existing literature on the use of HPP for alginate extraction, and no data have been reported regarding the physicochemical properties of the so-obtained alginates. The main hypothesis of this work was that HPP could increase the yield, inducing changes in the extracts' composition and structure, which will have an impact on its functional and technological applications. Therefore, the possibility of using HPP as a pre-treatment in the alginate extraction protocol has been evaluated also studying the effect of this pre-treatment on the composition, structure, and antioxidant capacity of the generated alginate-based extracts. Moreover, a detailed structural characterization of the different alginate gels produced by external gelation with $CaCl_2$ and of their mechanical performance was carried out using small angle X-ray scattering (SAXS), cryo-scanning electron microscopy (Cryo-SEM), and texture analysis.

2. Materials and methods

2.1. Materials

The brown seaweed *Ascophyllum nodosum* (*A. nodosum*) and *Saccharina latissima* (*S. latissima*) were supplied by Porto-Muiños S.L. (Cerceda, A Coruña, Spain) as a dry powder (< 2 % water content). Folin-Ciocalteu's reagent, sodium bicarbonate, hydrochloric acid (37 % (v/v)), gallic acid (≥98.0 % purity), Trolox (97 % purity), sodium hydroxide (pharma grade), $ABTS^{+\bullet}$ (HPLC grade), and commercial alginate (COM) (PHR1471) were supplied by Sigma-Aldrich (St. Louis, MO, USA).

2.2. Alginate extraction

Seaweeds *A. nodosum* and *S. latissima* were pre-treated using HPP and alginate extracted using the method described by Bojorges et al., 2022 to yield AHP and SHP alginate samples, respectively. Briefly, samples were dispersed in water, individually packed in sterile polyethylene bags, and heat-sealed using a liquid:solid ratio of 1:25 (wt.). Additionally, two overlapping bags were used to avoid any potential contact between the pressurizing fluid in the samples before being introduced into the High-Pressure Food Processor (EPSI NV, Belgium) vessel. HPP pre-treatment was carried out in a pilot-scale unit (2-liter vessel volume).

Based on previous literature in which the effect of HPP pre-treatment on polysaccharide extraction was optimized to reach higher extraction yields (Duan, Yan, Azarakhsh, Huang, & Wang, 2022), the samples were pressurized at 350 MPa, for 5 min at 20 ± 2 °C. The pressure level, pressurization time, and temperature were automatically controlled. After completing the pre-treatment, the samples were removed from the container and then submitted to the conventional extraction protocol, as previously described by Bojorges et al., 2022. Alginate extracts from *A. nodosum* and *S. latissima* were also obtained using the conventional protocol (without HPP pre-treatment; ACV and SCV, respectively), and commercial sodium alginate (COM; Sigma-Aldrich, PHR1471, Madrid, Spain) was further used for comparative purposes.

2.3. Characterization of alginate extracts

2.3.1. Proximate composition

The total nitrogen content of all the samples was analyzed using an Elemental Analyzer Rapid N Exceed (Paralab S.L., Spain). Approximately 250 mg of alginate samples were pressed into pellets and then analyzed using the Dumas method, which is based on the combustion of the sample and subsequent detection of the released N_2 (Wiles et al., 1998). The total protein content was determined from the nitrogen content multiplied by a factor of 5 (Angell, Mata, de Nys, & Paul, 2016). The determinations were carried out in triplicate.

The ash content was determined by dry biomass calcination of ca. 3 g of freeze-dried alginate and alginate-based fractions powder in a muffle furnace, according to the standard method (AOAC, 1990).

2.3.2. Determination of monosaccharide composition

The carbohydrate content and sugar composition of the fractions were determined in triplicate after acid methanolysis according to Bojorges et al., 2022, using high-performance anion-exchange chromatography with pulsed amperometric detection (HPAEC-PAD) with a Dionex ICS-6000 (ThermoFisher). In brief, the dry samples were incubated with 2 M HCl in dry methanol (1 mg/mL) at 100 °C for 5 h. Subsequently, samples were neutralized with pyridine, dried under a stream of air, and further hydrolyzed with 2 M TFA for 1 h at 120 °C. The samples were air-dried again and dissolved in water. Finally, the sample (4 mg) was incubated with 150 μL of 72 % H_2SO_4 for 3 h at room temperature; the solution was diluted with 1250 μL of deionized water and then incubated at 100 °C for 3 h. All experiments were carried out in triplicate.

2.3.3. $ABTS^{+\bullet}$ radical cation scavenging activity

The antioxidant capacity of the different alginate extracts was determined, in triplicate, using the Trolox equivalent antioxidant capacity, according to (Re et al., 1999) with some modifications described in Bojorges et al., 2022. Trolox (6-hydroxy-2,5,7,8-tetramethylchroman-2-carboxylic acid) was used as antioxidant standard.

2.3.4. Phenolic content

The total phenolic content was determined, in triplicate, by the Folin-Ciocalteau reagent as described by Singleton, Orthofer, and Lamuela-Raventós (1999) with a slight modification previously described in Bojorges et al., 2022. The calibration curve was generated by using gallic acid as the standard, and the total phenolic content was expressed as mg of gallic acid (GA)/g extract.

2.3.5. Fourier transform infrared spectroscopy (FT-IR)

Freeze-dried alginate powdered was analyzed by FT-IR (FTIR; Bruker, Vertex, USA) using the attenuated total reflectance (ATR) sampling method. The spectra were recorded at 4 cm^{-1} resolution in a wavelength range between 400 and 4000 cm^{-1} and averaging a

minimum of 64 scans.

2.3.6. Size exclusion chromatography (SEC)

The molar mass distribution of the alginate was analyzed by size exclusion chromatography (SECcurity 1260, Polymer Standard Services, Mainz, Germany coupled to a multiple-angle laser light scattering detector (MALLS; BIC-MwA7000, Brookhaven Instrument Corp., New York), and a refractive index detector (SECcurity 1260, Polymer Standard Services, Mainz, Germany) thermostated at 45 °C. The alginate solutions (1 mg/mL) were dissolved in 100 mM $NaNO_3$ with 5 mM NaN_3 and were filtered through a nylon filter (0.2 μm) prior to the analysis. Sample injections of 100 μL were performed into a combined column set-up with a SUPREMA pre-column, a SUPREMA 1000 Å, and two SUPREMA 3000 Å analytical columns (PSS, Mainz, Germany) eluting with 1 mL min^{-1} of 100 mM $NaNO_3$ with 5 mM sodium azide as mobile phase at 40 °C. The detailed procedure, calibration and setting parameters are detailed in the Supplementary Material.

2.3.7. Nuclear magnetic resonance (NMR) spectroscopy

^1H liquid-state NMR measurements were performed on a Bruker AV400 spectrometer operating at a frequency of 400 MHz for ^1H nuclei. The experiments were conducted with one single-pulse at 80 °C and the locked solvent to D_2O, recorded over a spectral width of 15 ppm during 4 s acquisition time, and 128 scans were collected. The M/G ratio and the diade/triade sequences were calculated from the area of ^1H NMR signals, according to Jensen, Larsen, and Engelsen (2015) and the equations are detailed in the Supplementary material.

2.3.8. Steady-shear flow measurements of alginate-based solutions

The rheological behavior of the alginate-based solutions was studied using a rotational rheometer (HAAKE Rheostress 1, Thermo Electric Corporation, Karlsruhe, Germany). Briefly, alginate solutions (2.5 %, w/v) were prepared, in triplicate, by dissolving the powered samples in deionized water. The shear stress (σ) was measured as a function of the shear rate ($\dot{\gamma}$) from 0 to 1000 s^{-1} at 25 ± 2 °C using a cone-plate geometry with a diameter of 35 mm and a gap of 54 μm. The power law model (Eq. 1) was applied to determine consistency index (k) and flow behavior index (n). Apparent viscosities were determined at 500 s^{-1}.

$$\sigma = \kappa \bullet \dot{\gamma}^{n} \quad (1)$$

Table 1
Proximal composition of alginate samples.

Composition (dry wt %)	ACV	AHP	SCV	SHP	COM
Yield	14.1 ± 0.4^{b}	23.0 ± 0.2^{c}	11.2 ± 0.4^{a}	13.9 ± 0.2^{b}	n/a
Protein	3.3 ± 0.3^{a,b}	2.8 ± 0.0^{a}	2.9 ± 0.3^{a}	3.6 ± 0.1^{b}	<0.1
Ash	19.4 ± 0.1^{b}	20.9 ± 0.1^{c}	21.3 ± 0.0^{d}	19.1 ± 0.1^{a}	20.0 ± 0.0^{c}
Carbohydrates[1]	68.8 ± 1.7^{a,b}	70.0 ± 1.8^{a,b}	68.0 ± 2.1^{a}	69.3 ± 1.7^{a,b}	72.0 ± 2.8^{b}
Of which[2]					
Fucose	2.8 ± 1.2^{b,c}	4.3 ± 1.1^{c}	1.1 ± 0.7^{b}	1.1 ± 0.7^{b}	<0.1^{a}
Xylose	1.9 ± 0.7^{b,c}	2.7 ± 0.8^{c}	0.2 ± 0.2^{a}	0.3 ± 0.3^{a}	1.1 ± 0.1^{a,b}
GulA	22.9 ± 0.7^{a}	24.2 ± 1.6^{a}	24.2 ± 1.6^{a}	25.3 ± 1.5^{a}	22.9 ± 1.7^{a}
GlcA	1.5 ± 0.2^{a}	1.2 ± 0.3^{a}	0.7 ± 1.0^{a}	0.6 ± 0.4^{a}	0.7 ± 0.7^{a}
ManA	39.6 ± 1.4^{a}	38.1 ± 1.8^{a}	40.8 ± 1.3^{a}	41.0 ± 2.3^{a}	45.3 ± 2.5^{b}
Polyphenols (mg GAE/g sample)	60.0 ± 2.5^{d}	67.6 ± 2.4^{e}	45.6 ± 1.4^{b}	56.2 ± 2.1^{c}	11.2 ± 1.4^{a}

The values report means (n = 3) ± standard deviation. For alginate samples, different letters in the same row indicate significant differences between the samples ($p < 0.05$).

[1] Total carbohydrate content calculated as the sum of all monosaccharides detected by HPAEC-PAD.

[2] Galactose, glucose, mannose and mannitol were detected in negligible amounts (<1 wt%) in all samples.

2.4. Development and characterization of alginate beads

The alginate beads were prepared by the syringe extrusion method. One mL of each alginate solution was extruded into a gelling bath containing 50 mM $CaCl_2$ solution. The distance between the tip and the gelling bath was set at 8 cm. The extruded gel particles were allowed to stand for 30 min for hardening, before being collected and rinsed with milli-Q water until testing.

The cationic composition (Ca^{2+} and Na^{+}) of the alginate beads was determined by inductively coupled plasma mass spectrometry (ICP-MS). The samples were subjected to an acid digestion in an oven at 200 °C and analyzed using an Agilent 7900 instrument.

2.4.1. Texture analysis

For the textural measurements, the alginate beads underwent uniaxial compression using a TA-XT Plus Texture Analyzer (Stable Micro Systems, UK) equipped with a 50 mm diameter cylindrical probe operating at a speed of 1 mm·s^{-1} and 80 % strain at ambient temperature (22 °C) (Krop, Hetherington, Holmes, Miquel, & Sarkar, 2019). Due to the size variation of the alginate beads, ten beads from each alginate extract were measured and replicated thrice (Ching, Bansal, & Bhandari, 2016).

2.4.2. Cryo-scanning electron microscopy

A JSM-5410 SEM microscope (JEOL, Tokyo, Japan) was used with a Cryo CT-1500C unit (Oxford Instruments, Witney, UK) for the Cryo-SEM observation. Alginate beads were placed in the holder and frozen in liquid nitrogen ($T \leq -210$ °C). Then, the samples were transferred to the cryostorage, fractured, etched at −90 °C for 15 min, and sputtered with a gold layer. Afterward, the samples were examined at −130 °C, 1.5 kV, and at a working distance of 15 mm in order to ensure high image resolution.

2.4.3. Small angle X-ray scattering (SAXS)

SAXS experiments were performed on the non-crystalline diffraction beamline, BL-11, at the ALBA synchrotron light source (www.albasynchrotron.es). The nanostructure of alginate solutions, before and after the addition of $CaCl_2$, was characterized by means of SAXS. The experimental procedure as well as data analysis were based on previous works from the co-authors (Gómez-Mascaraque et al., 2021; Gómez-Mascaraque, Martínez-Sanz, Hogan, López-Rubio, & Brodkorb, 2019). Aliquots of alginate solutions (containing 2.5 % alginate and 50 Mm $CaCl_2$) were placed in 2 mm sealed quartz capillaries (Hilgenberg Gmbh, Germany) and allowed to cool at 25 °C for 24 h to form gels prior to the experiments.

The energy of the incident photons was 12.4 keV or, equivalently, a wavelength, λ, of 1 Å. SAXS diffraction patterns were collected using a photon counting detector, Pilatus 1 M, with an active area of 168.7 × 179.4 mm^2, an effective pixel size of 172 × 172 μm^2 and a dynamic range of 20 bits. The sample-detector distance was set to 6425 mm, resulting in a q-range with a maximum value of q = 0.23 $Å^{-1}$. An exposure time of 2 s was selected based on preliminary tests. The data reduction was treated with the pyFAI python (ESRF) code (Kieffer & Wright, 2013), modified by the ALBA beamline staff, to make online azimuthal integrations from a previously calibrated file. Calibration files were created from a silver behenate (AgBh) standard. Intensity profiles were then plotted as a function of q using the IRENA macro suite (Ilavsky & Jemian, 2009) within the Igor software package (Wavemetrics, Lake Oswego, Oregon). A scattering background (corresponding to a quartz capillary filled with distilled water) was subtracted from all samples.

The scattering data were fitted to a unified model with two or three

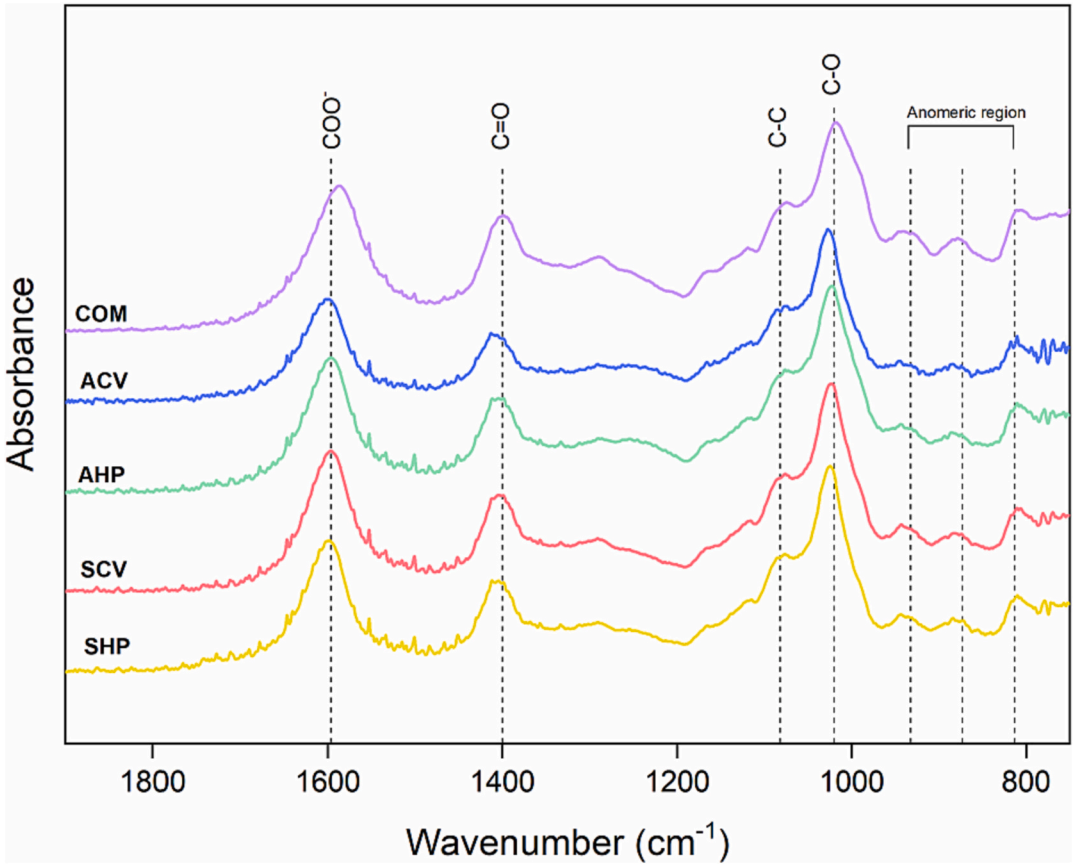

Fig. 1. FTIR spectra of alginate samples.

levels, depending on the sample:

$$I(q) = \sum_{i=1}^{N} G_i exp\left(-q^2 \bullet \frac{R_{g.i}^2}{3}\right) + \frac{B_i\left[erf\left(qR_{g.i}/\sqrt{6}\right)\right]^{3P_i}}{q^{P_i}} + bkg \quad (2)$$

This model considers that, for each individual level, the scattering intensity is the sum of a Guinier term and a power-law function (Beaucage, 1995). $G_i = c_i V_i \Delta SLD_i^2$ is the exponential prefactor (where V_i is the volume of the particle and ΔSLD_i is the scattering length density (SLD) contrast existing between the *i*th structural feature and the surrounding solvent), $R_{g,\,i}$ is the radius of gyration describing the average size of the *i*th level structural feature and B_i is a q-independent prefactor specific to the type of power-law scattering with power-law exponent, P_i.

2.5. Statistical analysis

The statistical analysis of experimental data was conducted using IBM SPSS Statistics software (version 23, IBM Corp., USA) through one-way analysis of variance (ANOVA). Tukey's test was used at a significance level of $p < 0.05$ for multiple comparison tests.

3. Results and discussion

3.1. Extraction yield and composition of the alginate extracts

In the first part of this work, the alginate extracts obtained by applying the HPP pre-treatment were characterized and compared with their counterparts prepared by means of the conventional method. The yield and composition of the extracts obtained from the two species were investigated and the results are compiled in Table 1. As observed, the alginate extraction yield of HPP pre-treated samples was 23 and 14 % for *A. nodosum* and *S. latissima*, respectively (Table 1), being significantly higher than their counterparts prepared with the conventional method. It is worth mentioning that the yield increase after the pre-treatment was substantially greater for *A. nodosum* pointing out that the high pressure applied was more effective in this case for causing cell wall disruption, resulting in a significant increase in the alginate yield. Similarly, the application of HPP has been reported to improve the extraction yield of polysaccharides and proteins from *P. palmata* and *S. chordalis*, respectively (Suwal et al., 2019). Furthermore, other intracellular compounds such as proteins, polyphenols (Jurić, Ferrari, Velikov, & Donsì, 2019), lipids (Imatoukene, Koubaa, Perdrix, Benali, & Vorobiev, 2020), and other bioactive compounds (Navarro-López, López-Rodríguez, Acién-Fernández, Molina-Grima, & Cerón-García, 2020) can be simultaneously extracted using HPP treatments, ascribed to the cell wall damage. In fact, the polyphenol content in HPP pre-treated samples significantly increased as compared to their counterparts prepared by means of the conventional methodology, evidencing that the cell wall disruption favors the co-extraction of phenolic compounds with alginate.

It should be highlighted that different seaweed species show very variable extraction yields and, not only the extraction conditions but also the harvest season and the environmental factors can significantly affect the yield (Okolie et al., 2020). In this work, the obtained alginate extraction yields using both extraction methodologies were among the highest reported in the literature, such as *C. barbata* (9.9 %) (Sellimi et al., 2015), *C. sedoides* (11 %) (Hadj Ammar, Hafsa, Le Cerf, Bouraoui, & Majdoub, 2016), *S. oligocystum* (18.9 %) (Davis, Ramirez, Mucci, & Larsen, 2004), *D. dichotoma* (20.94 %) and *S. fluitans* (21.1 %) (Parthiban, Parameswari, Saranya, Hemalatha, & Anantharaman, 2012), *S. angustifolium* (3.5 %) (Borazjani et al., 2017), and *C. compressa* (21.6 %) (Hentati et al., 2018).

The proximate composition, ash, and protein contents were also analyzed and the results are also shown in Table 1. The protein content did not significantly vary among samples. On the other hand, the ash

Table 2
Physicochemical properties of alginates extracts and COM.

Sample	M_w (kDa)	M_n (kDa)	Đ	v_g (–)
COM	68.34	19.24	3.55	0.63
ACV	241.90	157.40	1.54	0.66
AHP	179.70	115.20	1.56	0.67
SCV	169.40	74.74	2.27	0.64
SHP	257.30	148.60	1.73	0.73

The abbreviations M_w, M_n, and v_g denote the molecular weight, number molecular weight, dispersity, and fractal coefficient, respectively.

content results agreed with available literature in which an ~30 % ash was found in alginate extracts from *C. schiffneri* (Benslima et al., 2021). Polyphenols and proteins (5.9 mg/g) are also present in minor quantities in commercial food-grade sodium alginates (Dusseault et al., 2006). As expected, all the alginate extracts presented high polysaccharide contents, alginate units (mannuronic acid — ManA and guluronic acid — GulA) begin the main sugar constituents, followed by fucose, xylose and glucuronic acid (GlcA). The high alginate content in the extract was reflected by the sum of GulA and Man A units, which was around 62 wt% and 65–66 wt% for *A. nodosum* and *S. latissima*, respectively, and is in line with the purity of typical commercial alginates (COM). The relatively high purity of HPP pre-treated samples evidences that the higher yields were not the result of higher extraction of untargeted compounds (Deniaud-Bouët et al., 2017).

Considering that the alginate content in the raw seaweeds was 21.5 wt% and 25.4 wt% for *A. nodosum* and *S. latissima*, respectively (Bojorges et al., 2022), the HPP pre-treatment greatly promoted the extraction of alginate with high purity from both seaweeds. This was

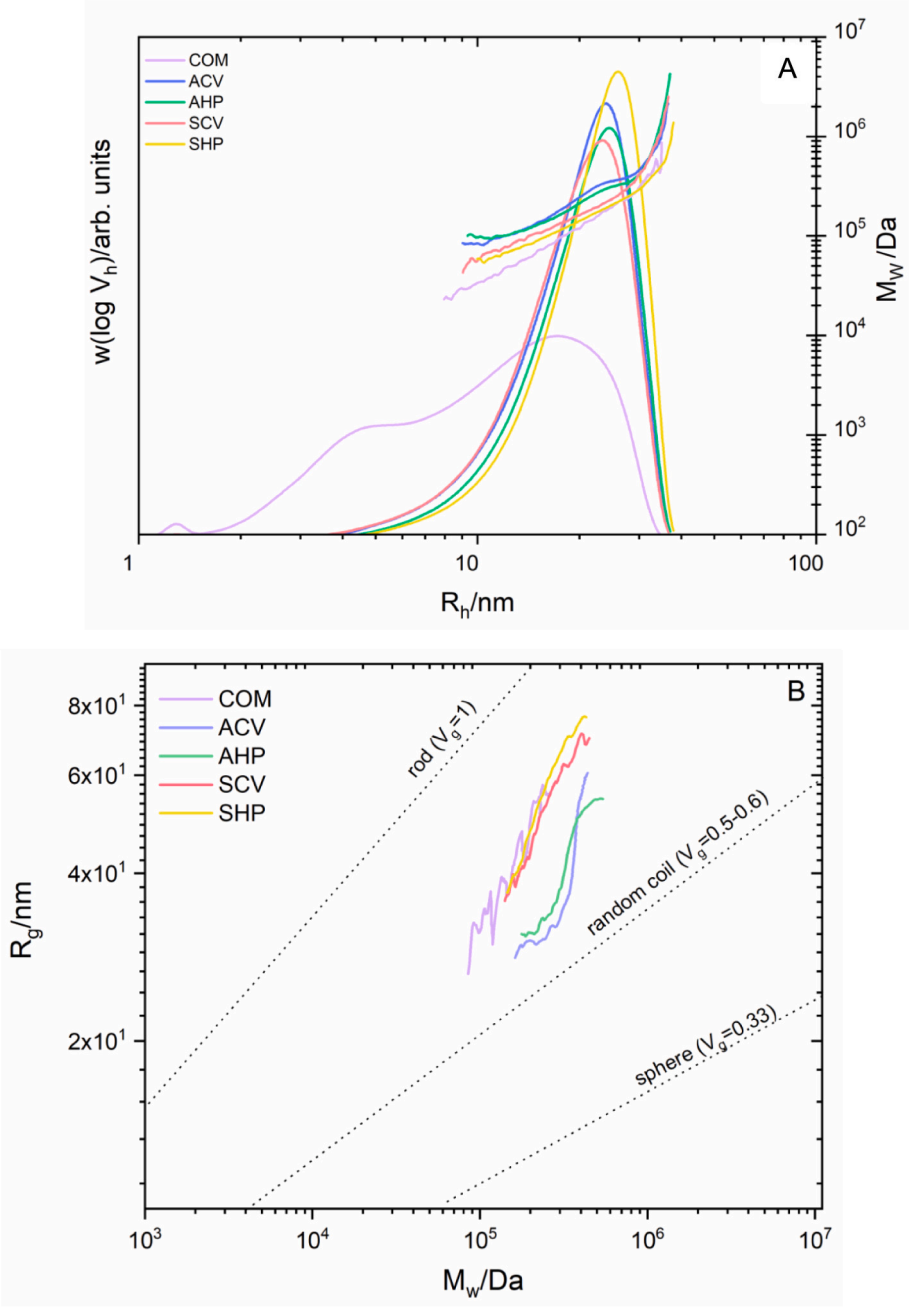

Fig. 2. (A) SEC molecular weight [w (log V_h)] and weight average molecular weight [M_w (V_h)] distributions of different alginates extracted, as function of the hydrodynamic radius of these samples, (B) fractal dimension v_g allows for assessing the alginate conformation.

more evident for *A. nodosum* in which 97.5 % of the alginate present in the raw seaweeds was extracted together with other components such as polyphenols and sulphated polysaccharides. This effect can be ascribed to the differences in the cell wall structure of both species (Deniaud-Bouët, Hardouin, Potin, Kloareg, & Hervé, 2017), and it may be interesting for the production of functional extracts as it will be described below. It is also worth noting that the use of HPP promo ted the extraction of fucose and xylose units from *A. nodosum*, highlighting the presence of sulphated fucoidan/fucan structures in the extract, in agreement with their higher abundance in the cell wall architecture of this family (Deniaud-Bouët et al., 2017). The alginate extracts were also qualitatively characterized by means of FT-IR, and the obtained spectra are shown in Fig. 1. As observed, the spectra were not significantly different to those from the commercial alginate, thus confirming the purity of the samples. This was reflected in the range between 800 and 1700 cm^{-1} in which the characteristic alginate bands could be identified. Specifically, the band at around 1600 cm^{-1}, corresponding to the asymmetric carbonyl stretching in the carboxylate anion (COO^{-}), the bands at 1100 and 1025 cm^{-1}, associated to the C—C and C—O stretching vibrations of the pyranose ring (Montes, Gisbert, Hinojosa, Sineiro, & Moreira, 2021) and the fingerprint or anomeric region (750–950 cm^{-1}) (Flórez-Fernández et al., 2019; Mohd Fauziee, Chang, Wan Mustapha, Md Nor, & Lim, 2021) described by the band observed at 918 cm^{-1} related to the C—O stretching vibration of the uronic acid residue, the band at 850 cm^{-1} associated with the C1—H deformation vibration of β-mannuronic acid, and the weak bands from 780 to 815 cm^{-1} assigned to the vibrations of mannuronic acid residues (Gómez-Ordóñez & Rupérez, 2011).

The weight average molecular weight (Mw), the number average molecular weight (Mn), the dispersity (Đ = Mw/Mn), and the radius of gyration (Rg) of the different alginate extracts and the reference (COM) were analyzed by means of SEC-MALLS, and the results are gathered in Table 2. Furthermore, Fig. 2a depicts the relative molar mass distribution of all samples. A single peak was clearly observed in all samples, except in the commercial one. As observed, the M_w of the different alginate extracts ranged between 169 and 257 kDa (see Table 2), while the commercial alginate was significantly lower (around 68 kDa). It should be highlighted that the dispersity for all the samples was >1, indicating high Mw dispersity, especially in the commercial one. According to the literature, the weight average molecular weight of commercial alginate from brown seaweeds ranges between 32 and 400 kDa (Rinaudo, 2007).

It is worth mentioning that the HPP pre-treatment significantly reduced the Mw values of the AHP samples as compared to its counterpart prepared with the conventional method. In contrast, this effect was not observed in SHP samples, which could be ascribed to the differences in chemical composition and cell wall structure and pointing out to more recalcitrant nature of the alginate from *S. latissima*.

It is well known that SEC alone separates grounded on hydrodynamic volume rather than molecular weight, with light scattering also allowing the assessment of chain conformation as represented by the fractal dimension ν_g, which occurs as an exponent in the de Gennes scaling law concept: $R_g = K_g(Mw)^{\nu g}$ (Marczynski et al., 2021). For COM and SCV alginates, the v_g adopts values of 0.63 and 0.64, respectively, corresponding to a random coil with a relatively flexible conformation. For the alginates extracted by the conventional method ACV and AHP, v_g values of 0.66 and 0.67 were obtained, respectively, which would indicate a slightly stiffer conformation, while for SHP the v_g was 0.73, which corresponded to an even stiffer conformation (Table 2, Fig. 2b). A more rigid polymeric chain conformation may contribute to the formation of stronger SHP hydrogels, as it will be detailed below.

The physical properties, the ability to form gels and the strength of the alginate gels depend not only on the molecular weight distribution, but also on the uronic acid composition and the relative properties of the three types of blocks. In fact, it is well-known that stronger gels can be formed with alginates with high guluronic acid content since the egg-box conformation is preferentially formed among G-sequences forming junctions with divalent cations (Chan et al., 2011; Mørch, Donati, Strand, & Skjåk-Bræk, 2006). Therefore, the monomeric sequences of the alginate extracts, and reference samples were also compared by NMR. The calculated M/G ratios as well as the monads (M and G), diades (MM, GG, MG), and triades (MGM, GGM, GGG), shown in Table 3, revealed great differences between them.

Table 3
Composition data and sequence parameters of alginates extracts and COM.

	Frequency[a]				
	ACV	AHP	SCV	SHP	COM
M	0.56	0.58	0.60	0.54	0.55
G	0.44	0.42	0.40	0.46	0.45
MM	0.40	0.41	0.41	0.36	0.34
GG	0.28	0.24	0.21	0.28	0.24
MG	0.16	0.18	0.19	0.18	0.21
MGM	0.15	0.14	0.11	0.14	0.10
GGM	0.02	0.04	0.08	0.04	0.11
GGG	0.25	0.20	0.13	0.27	0.13
M/G	1.8	1.9	2.1	1.6	2.3
$N_{G>1}$	14.50	7.00	3.63	7.00	8.00

M: β-D-mannuronic acid monomer; G: α-L-guluronic acid monomer. Mannuronate (M) and guluronate (G); $N_{G>1}$: average block length; M: M fraction; G: G fraction; MM: homopolymer fraction diads; GM: heteropolymer fraction diads; GGG and MMM homopolymer fraction triads; MGM and GGM: heteropolymer fraction triads.

[a] Expressed as molar fraction.

In general, the amount of heteropolymeric diad blocks (MG) was lower (around 0.16–0.21) than MM homopolymeric blocks (0.40–0.46), followed by GG (0.34–0.41). The content of GGM triades ranged between 0.02 and 0.11, MGM values were around 0.10–0.15, and GGG values ranged between 0.13 and 0.27.

M/G ratios and G-sequences of alginate extracts obtained from *S. latissima* by means of the conventional method and the commercial one, SCV and COM were very similar, whereas ACV presented lower M/G values and higher GG and GGG blocks, thus suggesting that ACV would give stronger gels, as it was later on confirmed. An important observation is that the HPP pre-treatment did not alter M/G values of the resulting AHP extracts, and a slight reduction in the G-sequences was noted. For the SHP extract, a lower M/G ratio was observed, the homopolymeric content of MM was significantly lower (0.36), while the GGG content (0.27) was clearly higher than in the non-pretreated extract or the other alginate extracts. It has been described that Ca^{+2} cations bind both to G sequences and to alternating GM and GGM dimeric/trimeric blocks but not to M-blocks only (Mørch et al., 2006), both being highest in SHP extracts.

Therefore, the HPP pre-treatment had a different effect on the alginate extraction depending on the recalcitrant nature of the algae and significant differences were observed between the two species. Alginate yield was significantly higher in those obtained from *A. nodosum* and the molecular weight was greatly affected (lower Mw values) by the HPP pre-treatment, probably ascribed to a partial degradation of the polymer chains. However, neither the M/G ratio nor the M and G sequences were greatly modified. In contrast, the more recalcitrant nature of *S. latissima* was patent on the lower increase in the extraction yield after the HPP pre-treatment (as compared to *A. nodosum*). In this case, the HPP pre-treatment resulted in an alginate with increased Mw and higher abundance of G-sequences, all of which will impact the molecular organization and technological performance.

3.2. Antioxidant capacity of the alginate extracts

Algae and seaweeds are known to contain bioactive compounds such as polyphenols and sulphated polysaccharides that possess antioxidant properties (Abdel-Latif et al., 2022). Therefore, the antioxidant capacity

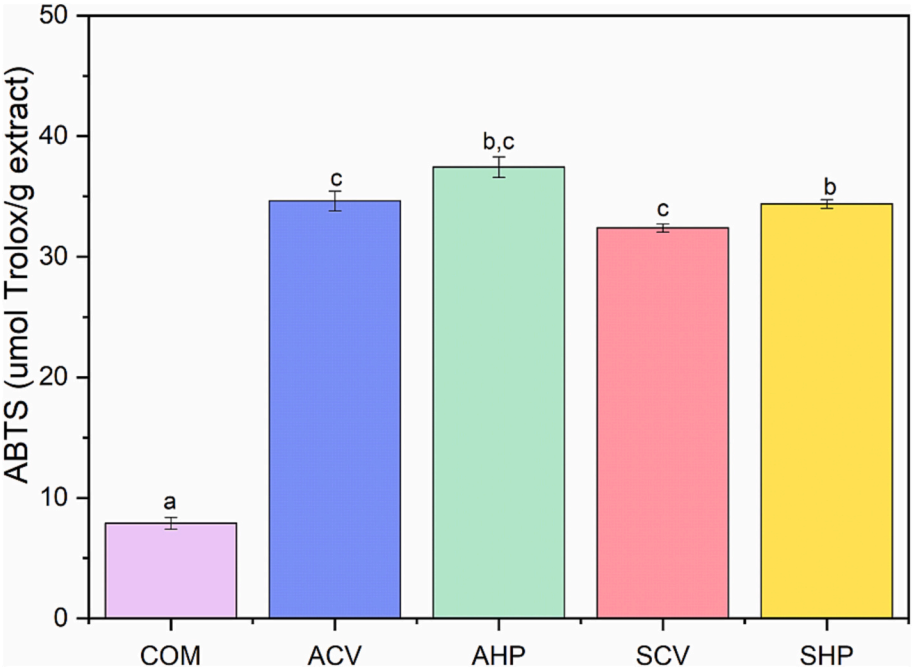

Fig. 3. Antioxidant capacity of the alginates determined by ABTS radical scavenging activity. Different letters indicate significant differences ($p < 0.05$).

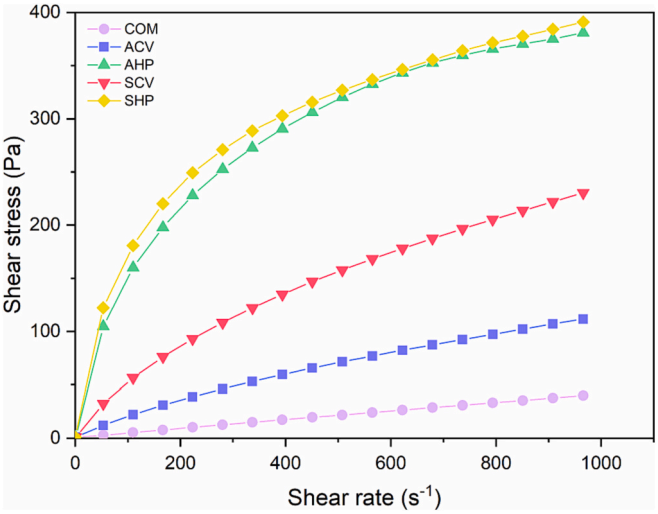

Fig. 4. Experimental (symbols) and fitted (lines) flow curves obtained by Ostwald de Waele model.

of the alginate-based extracts from both species was evaluated. As shown in Fig. 3, the alginate extracts showed higher antioxidant activity than the commercial one (COM). This can be ascribed to their higher polyphenol and protein content (see Table 1). In fact, several authors have reported that the antioxidant activity of macroalgae is related not only to the polyphenol content (Hardouin et al., 2014; Suwal et al., 2019), but also to the protein content and the presence of polysaccharide degradation products (Siriwardhana et al., 2008). It is worth mentioning that the antioxidant capacity was significantly higher for the AHP. This was already anticipated due to the higher polyphenol content, the lower molecular weight of the alginate and the presence of sulphated polysaccharides in the alginate-based extracts obtained from *A. nodosum* (Abka Khajouei et al., 2021). In fact, some works have demonstrated that alginates with lower molecular weight showed higher antioxidant activity (Kelishomi et al., 2016; Khajouei et al., 2018). Furthermore, other authors have shown that alternative extraction procedures (such as enzymatic and radiation methods) may provide antioxidant properties to the resulting alginate extract, ascribed to the alginate depolymerization (Falkeborg et al., 2014; Kelishomi et al., 2016; Zhao, Li, Xue, & Sun, 2012). Therefore, the lower molecular weight found in AHP sample could have also contributed to an increase on its antioxidant activity.

3.3. Rheological behavior of the different alginate-based extracts

Complete flow curves shown in Fig. 4 indicate that all the solutions presented a shear thinning behavior (pseudoplastic), which was more accentuated when the HPP pre-treatment was applied. The rheological data of pseudoplastic solutions were fitted to the Ostwald-de Waele model (Eq. 1). Table S1 gathers the flow (n) and consistency indexes (κ), together with the apparent viscosity (η_{ap}) values at the shear rate of 500 s^{-1}. The values of the correlation coefficient were in all cases around 0.99, evidencing that the rheological behavior of the alginate-based solutions was well-described by the power-law model, in agreement with the results found in literature (Abka Khajouei et al., 2021; Cevoli, Balestra, Ragni, & Fabbri, 2013; Hentati et al., 2020; Ma, Lin, Chen, Zhao, & Zhang, 2014). In fact, the rheological parameters and the apparent viscosity at 500 s^{-1} of the alginate extracts obtained using the conventional extraction protocol (ACV and SCV) were in the order of those found by Ma et al. (2014). It was clearly observed that the HPP pre-treatment (AHP and SHP) promoted significant changes in the rheological patterns of the alginate extracts, increasing the apparent viscosity and consistency index (*k*) and decreasing the flow index (n). These results indicate that AHP and SHP made the fluid solutions more viscous and more shear thinning, probably due to the formation of different intermolecular entanglements (Montes et al., 2021), which is greatly influenced by the molecular weight of the biopolymers (higher M_w values for SHP) and the presence of other low molecular weight compounds (such as polyphenols).

3.4. Alginate-based hydrogels

The four alginate extracts and the commercial one were used to produce hydrogels with the addition of $CaCl_2$. Fig. 5A shows representative cross-section micrographs of the corresponding beads. As

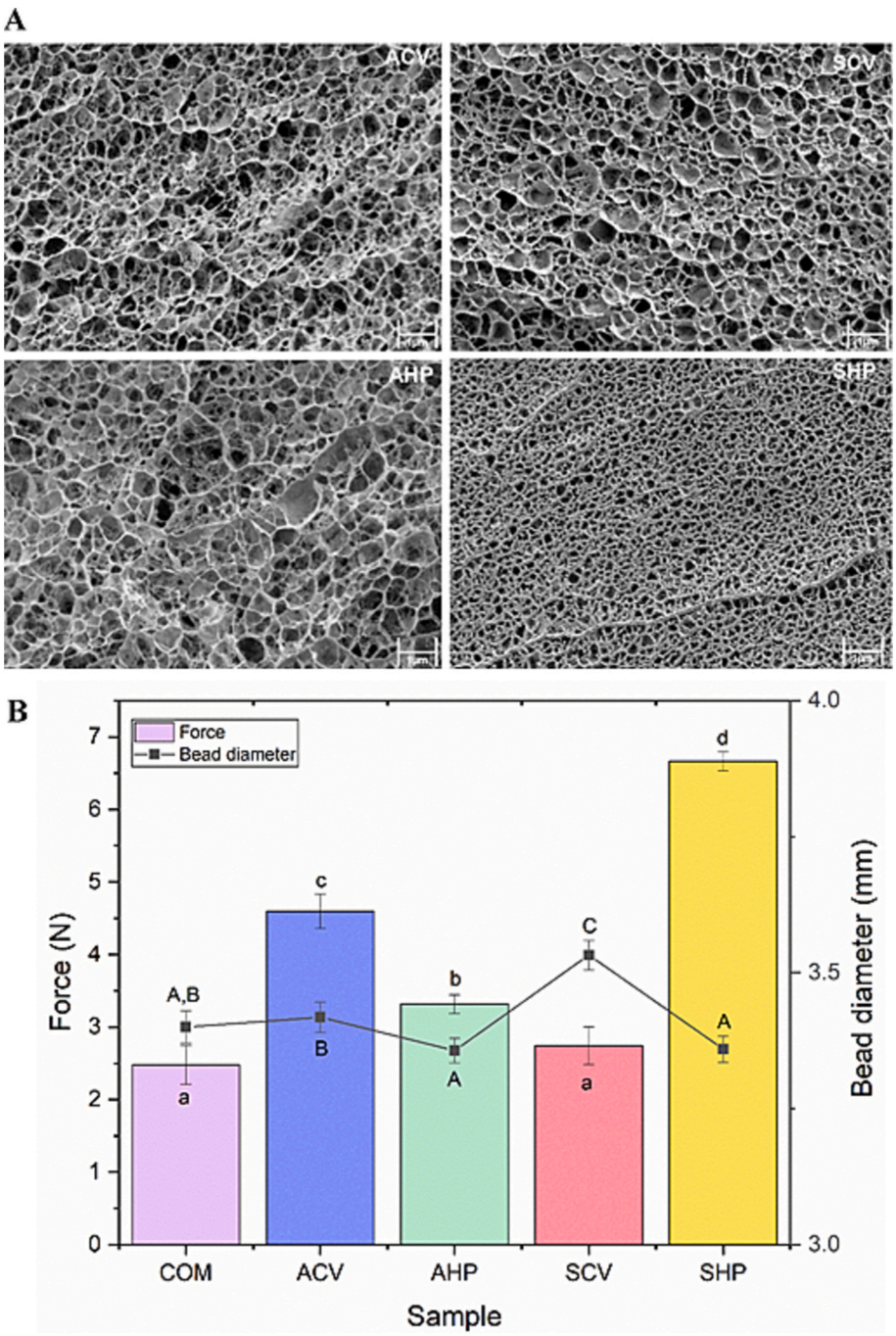

Fig. 5. (A) Cryo-SEM micrographs of alginate beads (B) Comparison of maximum force and average alginate bead diameter. Different lowercase letters indicate significant differences ($p < 0.05$) in the force of the alginate beads. Different uppercase letters indicate significant differences ($p < 0.05$) in bead diameter.

observed, a less compact network was found in hydrogel capsules prepared with alginate extracts from *A. nodosum*, being the pore size greater than in their counterparts prepared with *S. latissima*. This effect could be ascribed to the presence of other components which could interfere in the gelation process of the alginate. Interestingly, the effect that the HPP pre-treatment had on the microstructure of the hydrogel capsules depended on the raw material used. It was clearly observed that in the alginate from *S. latissima* the pre-treatment promoted the formation of a denser structure with a decrease in the average pore size, in agreement with the SAXS results (Fig. 6).

The gel strength of the obtained hydrogel capsules from the different alginate extracts was evaluated by means of uniaxial compression tests. Fig. 5B summarizes the calculated gel strength values for the alginate-based capsules. The first thing to highlight is that the application of HPP pre-treatment significantly improved the gel strength of SHP. This improvement can be related to a higher molecular weight, a slightly lower M/G ratio (Tables 1 and 3), especially, to a stronger presence of G blocks (GG and GGG; Table 3). In contrast, the gel strength of AHP was significantly decreased as compared to ACV, fact which can be related to the lower molecular weight of the AHP, the presence of other low molecular weight compounds which could interfere in the gelation mechanism and the lower abundance of G blocks (Table 3). Furthermore, these results agreed with the conformation results for alginate molecules already presented in Table 2. As it was anticipated, AHP alginates showed the most flexible linear conformation whereas SHP samples comprised a stiffer conformation.

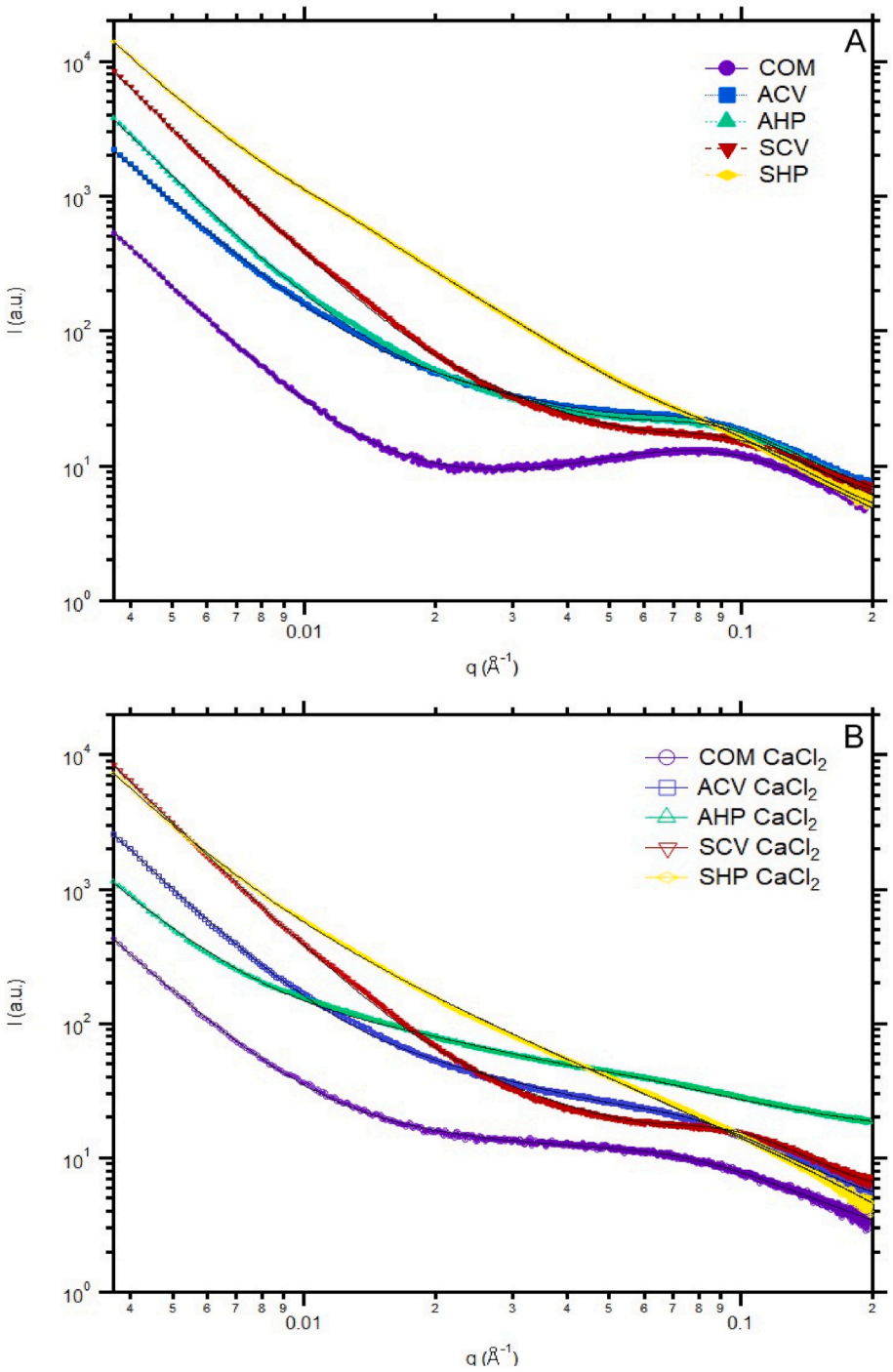

Fig. 6. SAXS patterns from (A) the 2.5 % w/v alginate solutions and (B) the same samples after the addition of 50 mM $CaCl_2$. Markers correspond to the experimental data and black solid lines represent the fitting curves.

To further investigate structural differences between the various hydrogels, the amount of Ca^{2+} in the developed capsules was also determined since the stiffness of alginate beads not only depends on alginate concentration and composition, M/G ratio, and the alternating M and G blocks, but is also affected by the degree of crosslinking. To confirm that, the cationic composition of all the alginate beads was determined by means of ICP-MS to quantify the amounts of Na^{+} and Ca^{2+}. The results, compiled in Table S2, evidence Ca^{2+} as the most abundant cation in SHP and AHP hydrogels, its concentration increasing with HPP pre-treatment compared to SCV and ACV. However, an opposite tendency was observed with sodium, this increasing in AHP and decreasing in SHP. The higher Ca^{2+} is consistent with the structural properties of the alginate extracts (Mørch et al., 2006).

3.5. SAXS characterization of the alginates and alginate hydrogels

The nanostructure of the alginate aqueous solutions, before and after the addition of $CaCl_2$ to induce the association of alginate chains and promote the formation of gels, was investigated by means of small angle X-ray scattering (SAXS) and the obtained scattering patterns are shown in Fig. 6. As observed, most of the samples were characterized by the appearance of a broad scattering peak within the high q region, being

Table 4
Parameters obtained from the fits of the SAXS data from the alginate solutions before and after the addition of $CaCl_2$ (Rg_i: radius of gyration for the structural level *i*; P_i: power-law exponent for the structural level *i*).

	P_1	Rg_2 (nm)	P_2	Rg_3 (nm)	P_3
COM	–	–	3.1	3.6	1.2
COM $CaCl_2$	–	–	2.9	4.8	1.2
ACV	–	–	2.9	3.8	2.3
ACV $CaCl_2$	–	–	3.0	4.3	2.0
AHP	–	–	3.1	3.6	2.7
AHP $CaCl_2$	–	–	2.9	8.1	1.0
SCV	–	–	3.1	3.3	3.1
SCV $CaCl_2$	–	–	3.0	3.4	2.6
SHP	3.6	37.1	2.3	4.5	2.1
SHP $CaCl_2$	–	–	3.0	12.6	1.4

this feature more evident in the solution of the commercial alginate. On the contrary, this feature was not visible in the SHP alginate (i.e. the extract with the highest Mw). Interestingly, the intensity of this peak was reduced when $CaCl_2$ was added to the solutions, being the difference between the solutions before and after $CaCl_2$ addition more obvious in the commercial alginate and the *A. nodosum* alginates. Similar scattering peaks have been detected in the SAXS patterns from commercial carrageenan hydrogels; however, the peaks were no longer visible when KCl was incorporated into the formulations (Fontes-Candia, Ström, Lopez-Sanchez, López-Rubio, & Martínez-Sanz, 2020). Furthermore, this scattering peak has not been reported for alginate gels produced by the addition of $CaCl_2$ (Gómez-Mascaraque et al., 2019). Fitting models based on cylindrical form factors or their sum with a power-law model (to account for the scattering intensity within the low q region) did not provide satisfactory fits for the experimental data. Thus, it is not expected that this peak arises from the form factor of the alginate molecular chains. In the absence of salts, the repulsion between negative changes may lead to the formation of extended molecular chains with a rod-like conformation; however, the neutralization of some of these negative charges would lead to ionic interactions, producing entangled networks. Accordingly, the scattering feature may correspond to an interference peak from the distance between adjacent polymeric chains within aggregates formed as a result of the presence of Na^+ cations neutralizing the negative charges in the alginate molecular chains.

The experimental data were fitted using an empirical Beaucage model (also known as unified model), which is described by the following mathematical equation:

$$I(q) = \sum_{i=1}^{N} G_i exp\left(-q^2 \bullet \frac{R_{g,i}^2}{3}\right) + \frac{B_i\left[erf\left(qR_{g,i}/\sqrt{6}\right)\right]^{3P_i}}{q^{P_i}} + bkg \quad (2)$$

This model considers that, for each individual level (i), the scattering intensity is the sum of a Guinier term and a power-law function (Beaucage, 1995). $G_i = c_i V_i \Delta SLD_i^2$ is the exponential prefactor (where V_i is the volume of the particle and ΔSLD_i is the scattering length density (SLD) contrast existing between the *i*th structural feature and the surrounding solvent), $R_{g,\,i}$ is the radius of gyration describing the average size of the *i*th level structural feature and B_i is a q-independent prefactor specific to the type of power-law scattering with power-law exponent, P_i. In the specific case of this study, all the data could be fitted using two levels, except for the data corresponding to SHP, in which case an additional level was required to account for the appearance of a weak shoulder-like feature within the mid-q region (see Fig. S2).

As deduced from the obtained fitting parameters, gathered in Table 4, the scattering intensity within the low q region could be described by a power-law function with exponents of ca. 2.9–3.1. This suggests the existence of highly clustered networks within the corresponding size range (170–70 nm). In the particular case of the alginate samples, the implication of this is that the alginate molecular chains are entangled forming highly branched networks due to inter-/intramolecular interactions. Thus, a greater P_2 exponent indicates a greater clustering degree in the sample. From all the samples, only SHP presented a lower P_2 exponent, suggesting that the degree of chain association was more limited in that case.

The radius of gyration associated to the scattering peak, related to the distance between adjacent molecular chains within the clusters, corresponded to 3.3–12.6 nm and, in general, the size increased with the addition of $CaCl_2$. This suggests the existence of surface fractals within the corresponding size range (170–70 nm), i.e. highly branched networks. The radius of gyration associated to the scattering peak corresponded to 3.3–12.6 nm and, in general, the size increased with the addition of $CaCl_2$. This suggests that, as commented before, in the presence of a certain amount of Na^+ cations the polysaccharide chains are intertwined, with small distances of 3–5 nm between adjacent chains. The addition of Ca^{2+} cations displaces Na^+ cations and promotes the formation of different structures, where the polysaccharide chains are more extended in a rod-like conformation. In fact, the addition of $CaCl_2$ produced a decrease in the power-law exponent corresponding to the high q region (P_3), reaching values close to 1 (corresponding to rigid rods) in some of the samples. In contrast, the samples before the addition of $CaCl_2$ generally presented P_3 values of 2–3, corresponding to mass

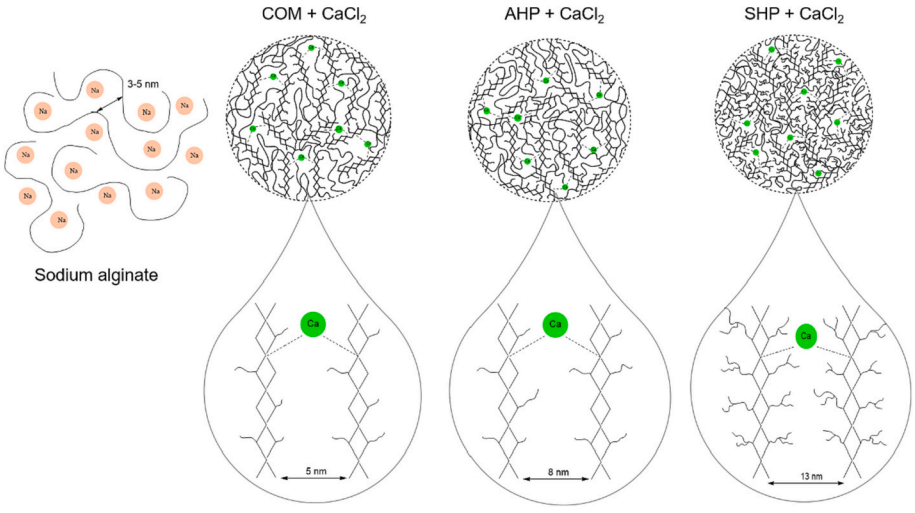

Fig. 7. Schematic representation for alginate hydrogels proposed for those obtained with high-pressure pre-treatment (AHP and SHP) and the commercial one (COM).

fractals, i.e. structures containing branching to form a 3D network. A greater P_3 exponent implies a greater deviation from the rigid rod-like behavior and indicates that the alginate chains are less linear and more entangled. This deviation from the rigid rod-like behavior was more notable in the SCV and AHP samples. Fig. 7 shows a schematic representation of the nanostructure of hydrogels formed with AHP, SHP and COM, as deduced from the SAXS results. It is worth noting that at the $CaCl_2$ concentration added in these experiments, it looks like egg-box structures were not abundant in the samples, and thus an associated correlation peak was not detected.

4. Conclusions

HPP pre-treatment was applied for the production of alginate-based extracts from *S. latissima* and *A. nodosum* (SHP and AHP, respectively) and compared to those obtained using the conventional extraction protocol (SCV and ACV). The HPP pre-treatment was able to effectively increase alginate yields, especially in *A. nodosum*, without compromising the purity. The higher polyphenol content in HPP pre-treated samples conferred them a relatively high antioxidant activity (35–38 μmol TE/g extract), being higher in AHP samples due to the presence of sulphated polysaccharides (fucoidan). The AHP extracts presented lower Mw than their ACV counterparts which could be ascribed to a partial depolymerization of the alginate during the extraction process. It also formed softer gels, owed to the lower Mw and less abundance of G-blocks. In contrast, *S. latissima*, the pre-treatment increased both the abundance of G-blocks and the Mw of the resulting polysaccharide. This explained the higher viscosity of the corresponding solutions and the stronger hydrogels formed in this case.

The nanostructure showed that the addition of Ca^{2+} promotes the formation of different structures, where the polysaccharide chains are more extended in a rod-like conformation. The deviation from the rigid rod-like behavior was more notable for SCV and AHP samples, indicating that the alginate chains are less linear and more entangled. Furthermore, at the $CaCl_2$ concentration used in these experiments, the well-reported egg-box structures were not abundant in the samples.

These results reveal differences in the cell wall architecture of the two algae families which directly affect the structural properties of the obtained alginates and the corresponding functional (antioxidant) and technological (rheological) properties (gelling or/and thickening). These evidence the potential of the HPP pre-treatment as an efficient path towards a better utilization of marine sources, with a potential improvement on the technological or functional properties of the alginates obtained, depending on the source.

CRediT authorship contribution statement

Hylenne Bojorges: Methodology, Investigation, Writing - original draft. A. Martínez-Abad: Methodology, Supervision, Writing - review & editing; M. Martínez-Sanz: Methodology, Investigation, Writing - review & editing, María Dolores Rodrigo: Methodology, Francisco Vilaplana: Methodology, Supervision, Writing - review & editing A. López-Rubio: Conceptualization, Methodology, Supervision, Funding acquisition, Project administration, Writing- Review. M.J. Fabra: Conceptualization, Methodology, Supervision, formal analysis, Funding acquisition, Writing- Review.

Declaration of competing interest

The authors declare that there are no conflicts of interest.

Data availability

Data will be made available on request.

Acknowledgments

Grants RTI-2018-094268-B-C22 and PID2020-117744RJ-I00 funded by MCIN/AEI/10.13039/501100011033 and, as appropriate, by "ERDF A way of making Europe", by the "European Union" or by the "European Union NextGenerationEU/PRTR". H. Bojorges acknowledges financial support from the Generalitat Valenciana for the award of a Santiago Grisolía grant (GRISOLIAP/2019/007).

Appendix A. Supplementary data

Supplementary data to this article can be found online at https://doi.org/10.1016/j.carbpol.2022.120175.

References

Abdel-Latif, H. M. R., Dawood, M. A. O., Alagawany, M., Faggio, C., Nowosad, J., & Kucharczyk, D. (2022). Health benefits and potential applications of fucoidan (FCD) extracted from brown seaweeds in aquaculture: An updated review. *Fish & Shellfish Immunology, 122*, 115–130. https://doi.org/10.1016/J.FSI.2022.01.039

Abka Khajouei, R., Keramat, J., Hamdami, N., Ursu, A. V., Delattre, C., Gardarin, C., Lecerf, D., Desbrières, J., Djelveh, G., & Michaud, P. (2021). Effect of high voltage electrode discharge on the physicochemical characteristics of alginate extracted from an Iranian brown seaweed (Nizimuddinia zanardini). *Algal Research, 56*, Article 102326. https://doi.org/10.1016/J.ALGAL.2021.102326

Angell, A. R., Mata, L., de Nys, R., & Paul, N. A. (2016). The protein content of seaweeds: A universal nitrogen-to-protein conversion factor of five. *Journal of Applied Phycology, 28*(1), 511–524. https://doi.org/10.1007/S10811-015-0650-1/FIGURES/5

AOAC. (1990). *Official methods of analysis of the Association of Official Analytical Chemists* (9th ed.). Association of Official Analytical Chemists.

Balboa, E. M., Moure, A., & Domínguez, H. (2015). Valorization of Sargassum muticum biomass according to the biorefinery concept. *Marine Drugs, 13*(6), 3745–3760. https://doi.org/10.3390/MD13063745

Beaucage, G. (1995). Approximations leading to a unified Exponential/Power-law approach to small-angle scattering. *Journal of Applied Crystallography, 28*(6), 717–728. https://doi.org/10.1107/S0021889895005292

Benslima, A., Sellimi, S., Hamdi, M., Nasri, R., Jridi, M., Cot, D., Li, S., Nasri, M., & Zouari, N. (2021). The brown seaweed Cystoseira schiffneri as a source of sodium alginate: Chemical and structural characterization, and antioxidant activities. *Food Bioscience, 40*, Article 100873. https://doi.org/10.1016/J.FBIO.2020.100873

Bojorges, H., Fabra, M. J., López-Rubio, A., & Martínez-Abad, A. (2022). Alginate industrial waste streams as a promising source of value-added compounds valorization. *Science of the Total Environment, 838*, Article 156394. https://doi.org/10.1016/J.SCITOTENV.2022.156394

Borazjani, N. J., Tabarsa, M., You, S., & Rezaei, M. (2017). Effects of extraction methods on molecular characteristics, antioxidant properties and immunomodulation of alginates from Sargassum angustifolium. *International Journal of Biological Macromolecules, 101*, 703–711. https://doi.org/10.1016/J.IJBIOMAC.2017.03.128

Brownlee, I. A., Allen, A., Pearson, J. P., Dettmar, P. W., Havler, M. E., Atherton, M. R., & Onsøyen, E. (2005). Alginate as a source of dietary fiber. *Critical Reviews in Food Science and Nutrition, 45*(6), 497–510. https://doi.org/10.1080/10408390500285673

Cevoli, C., Balestra, F., Ragni, L., & Fabbri, A. (2013). Rheological characterisation of selected food hydrocolloids by traditional and simplified techniques. *Food Hydrocolloids, 33*(1), 142–150. https://doi.org/10.1016/J.FOODHYD.2013.02.022

Chan, E.-S., Lim, T.-K., Voo, W.-P., Pogaku, R., Tey, B. T., & Zhang, Z. (2011). Effect of formulation of alginate beads on their mechanical behavior and stiffness. *Particuology, 9*(3), 228–234. https://doi.org/10.1016/j.partic.2010.12.002

Ching, S. H., Bansal, N., & Bhandari, B. (2016). Rheology of emulsion-filled alginate microgel suspensions. *Food Research International, 80*, 50–60. https://doi.org/10.1016/J.FOODRES.2015.12.016

Davis, T. A., Ramirez, M., Mucci, A., & Larsen, B. (2004). Extraction, isolation and cadmium binding of alginate from Sargassum spp. *Journal of Applied Phycology, 16*(4), 275–284. https://doi.org/10.1023/B:JAPH.0000047779.31105.EC

Deniaud-Bouët, E., Hardouin, K., Potin, P., Kloareg, B., & Hervé, C. (2017). A review about brown algal cell walls and fucose-containing sulfated polysaccharides: Cell wall context, biomedical properties and key research challenges. *Carbohydrate Polymers, 175*, 395–408. https://doi.org/10.1016/J.CARBPOL.2017.07.082

Duan, H., Yan, X., Azarakhsh, N., Huang, X., & Wang, C. (2022). Effects of high-pressure pretreatment on acid extraction of pectin from pomelo peel. *International Journal of Food Science & Technology, 57*(8), 5239–5249. https://doi.org/10.1111/IJFS.15840

Dusseault, J., Tam, S. K., Ménard, M., Polizu, S., Jourdan, G., Yahia, L., & Hallé, J.-P. (2006). Evaluation of alginate purification methods: Effect on polyphenol, endotoxin, and protein contamination. *Journal of Biomedical Materials Research Part A, 76A*(2), 243–251. https://doi.org/10.1002/jbm.a.30541.

Falkeborg, M., Cheong, L. Z., Gianfico, C., Sztukiel, K. M., Kristensen, K., Glasius, M., Xu, X., & Guo, Z. (2014). Alginate oligosaccharides: Enzymatic preparation and antioxidant property evaluation. *Food Chemistry, 164*, 185–194. https://doi.org/10.1016/J.FOODCHEM.2014.05.053

Fertah, M., Belfkira, A., Dahmane, Montassir, E., Taourirte, M., & Brouillette, F. (2017). Extraction and characterization of sodium alginate from Moroccan Laminaria digitata brown seaweed. *Arabian Journal of Chemistry, 10*, S3707–S3714. https://doi.org/10.1016/J.ARABJC.2014.05.003

Flórez-Fernández, N., Domínguez, H., & Torres, M. D. (2019). A green approach for alginate extraction from Sargassum muticum brown seaweed using ultrasound-assisted technique. *International Journal of Biological Macromolecules, 124*, 451–459. https://doi.org/10.1016/j.ijbiomac.2018.11.232

Fontes-Candia, C., Ström, A., Lopez-Sanchez, P., López-Rubio, A., & Martínez-Sanz, M. (2020). Rheological and structural characterization of carrageenan emulsion gels. *Algal Research, 47*, Article 101873. https://doi.org/10.1016/J.ALGAL.2020.101873

Gomez, L. P., Alvarez, C., Zhao, M., Tiwari, U., Curtin, J., Garcia-Vaquero, M., & Tiwari, B. K. (2020). Innovative processing strategies and technologies to obtain hydrocolloids from macroalgae for food applications. In *, 248*. *Carbohydrate Polymers* (p. 116784). Elsevier Ltd.. https://doi.org/10.1016/j.carbpol.2020.116784

Gómez-Mascaraque, L., Martínez-Sanz, M., Hogan, S. A., López-Rubio, A., & Brodkorb, A. (2019). Nano- and microstructural evolution of alginate beads in simulated gastrointestinal fluids. Impact of M/G ratio, molecular weight and pH. *Carbohydrate Polymers, 223*, Article 115121. https://doi.org/10.1016/J.CARBPOL.2019.115121

Gómez-Mascaraque, L., Martínez-Sanz, M., Martínez-López, R., Martínez-Abad, A., Panikuttira, B., López-Rubio, A., Tuohy, M. G., Hogan, S. A., & Brodkorb, A. (2021). Characterization and gelling properties of a bioactive extract from Ascophyllum nodosum obtained using a chemical-free approach. *Current Research in Food Science, 4*, 354–364. https://doi.org/10.1016/J.CRFS.2021.05.005

Gómez-Ordóñez, E., & Rupérez, P. (2011). FTIR-ATR spectroscopy as a tool for polysaccharide identification in edible brown and red seaweeds. *Food Hydrocolloids, 25*(6), 1514–1520. https://doi.org/10.1016/j.foodhyd.2011.02.009

Hadj Ammar, H., Hafsa, J., Le Cerf, D., Bouraoui, A., & Majdoub, H. (2016). Antioxidant and gastroprotective activities of polysaccharides from the Tunisian brown algae (Cystoseira sedoides). *Journal of the Tunisian Chemical Society, 18*, 80–88.

Hardouin, K., Burlot, A. S., Umami, A., Tanniou, A., Stiger-Pouvreau, V., Widowati, I., Bedoux, G., & Bourgougnon, N. (2014). Biochemical and antiviral activities of enzymatic hydrolysates from different invasive french seaweeds. *Journal of Applied Phycology, 26*(2), 1029–1042. https://doi.org/10.1007/s10811-013-0201-6

Hentati, F., Delattre, C., Ursu, A. V., Desbrières, J., Le Cerf, D., Gardarin, C., Abdelkafi, S., Michaud, P., & Pierre, G. (2018). Structural characterization and antioxidant activity of water-soluble polysaccharides from the Tunisian brown seaweed Cystoseira compressa. *Carbohydrate Polymers, 198*, 589–600. https://doi.org/10.1016/j.carbpol.2018.06.098

Hentati, F., Pierre, G., Ursu, A. V., Vial, C., Delattre, C., Abdelkafi, S., & Michaud, P. (2020). Rheological investigations of water-soluble polysaccharides from the Tunisian brown seaweed Cystoseira compressa. *Food Hydrocolloids, 103*, Article 105631. https://doi.org/10.1016/J.FOODHYD.2019.105631

Ilavsky, J., & Jemian, P. R. (2009). Urn:Issn:0021-8898. In *, 42. Irena: tool suite for modeling and analysis of small-angle scattering* (pp. 347–353). https://doi.org/10.1107/S0021889809002222 (2).

Imatoukene, N., Koubaa, M., Perdrix, E., Benali, M., & Vorobiev, E. (2020). Combination of cell disruption technologies for lipid recovery from dry and wet biomass of yarrowia lipolytica and using green solvents. *Process Biochemistry, 90*, 139–147. https://doi.org/10.1016/J.PROCBIO.2019.11.011

Jensen, H. M., Larsen, F. H., & Engelsen, S. B. (2015). Characterization of alginates by nuclear magnetic resonance (NMR) and vibrational spectroscopy (IR, NIR, Raman) in combination with chemometrics. *Methods in Molecular Biology, 1308*, 347–363. https://doi.org/10.1007/978-1-4939-2684-8_22

Jurić, S., Ferrari, G., Velikov, K. P., & Donsì, F. (2019). High-pressure homogenization treatment to recover bioactive compounds from tomato peels. *Journal of Food Engineering, 262*, 170–180. https://doi.org/10.1016/J.JFOODENG.2019.06.011

Kadam, S. U., & Prabhasankar, P. (2010). Marine foods as functional ingredients in bakery and pasta products. *Food Research International, 43*(8), 1975–1980. https://doi.org/10.1016/J.FOODRES.2010.06.007

Karaki, N., Sebaaly, C., Chahine, N., Faour, T., Zinchenko, A., Rachid, S., & Kanaan, H. (2013). The antioxidant and anticoagulant activities of polysaccharides isolated from the brown algae Dictyopteris polypodioides growing on the Lebanese coast. *Journal of Applied Pharmaceutical Science, 3*(2), 43–51. https://doi.org/10.7324/JAPS.2013.30208

Kelishomi, Z. H., Goliaei, B., Mahdavi, H., Nikoofar, A., Rahimi, M., Moosavi-Movahedi, A. A., Mamashli, F., & Bigdeli, B. (2016). Antioxidant activity of low molecular weight alginate produced by thermal treatment. *Food Chemistry, 196*, 897–902. https://doi.org/10.1016/j.foodchem.2015.09.091

Khajouei, R. A., Keramat, J., Hamdami, N., Ursu, A.-V., Delattre, C., Laroche, C., Gardarin, C., Lecerf, D., Desbrières, J., Djelveh, G., & Michaud, P. (2018). Extraction and characterization of an alginate from the Iranian brown seaweed nizimuddinia zanardini. *International Journal of Biological Macromolecules, 118*, 1073–1081. https://doi.org/10.1016/J.IJBIOMAC.2018.06.154

Kieffer, J., & Wright, J. P. (2013). PyFAI: A python library for high performance azimuthal integration on GPU. *Powder Diffraction, 28*(S2), S339–S350. https://doi.org/10.1017/S0885715613000924

Krop, E. M., Hetherington, M. M., Holmes, M., Miquel, S., & Sarkar, A. (2019). On relating rheology and oral tribology to sensory properties in hydrogels. *Food Hydrocolloids, 88*, 101–113. https://doi.org/10.1016/J.FOODHYD.2018.09.040

Łabowska, M. B., Michalak, I., & Detyna, J. (2019). Methods of extraction, physicochemical properties of alginates and their applications in biomedical field - A review. *Open Chemistry, 17*(1), 738–762. https://doi.org/10.1515/chem-2019-0077

Ma, J., Lin, Y., Chen, X., Zhao, B., & Zhang, J. (2014). Flow behavior, thixotropy and dynamical viscoelasticity of sodium alginate aqueous solutions. *Food Hydrocolloids, 38*, 119–128. https://doi.org/10.1016/J.FOODHYD.2013.11.016

Malafronte, L., Yilmaz-Turan, S., Krona, A., Martinez-Sanz, M., Vilaplana, F., & Lopez-Sanchez, P. (2021). Macroalgae suspensions prepared by physical treatments: Effect of polysaccharide composition and microstructure on the rheological properties. *Food Hydrocolloids, 120*, Article 106989. https://doi.org/10.1016/J.FOODHYD.2021.106989

Marczynski, M., Jiang, K., Blakeley, M., Srivastava, V., Vilaplana, F., Crouzier, T., & Lieleg, O. (2021). Structural alterations of mucins are associated with losses in functionality. *Biomacromolecules, 22*(4), 1600–1613. https://doi.org/10.1021/ACS.BIOMAC.1C00073/ASSET/IMAGES/LARGE/BM1C00073_0008.JPEG

Marin, C., Ibañez, D., Rios-Corripio, G., Guerrero, J. A., Rodrigo, D., & Martinez, A. (2020). Nature of the inactivation by high hydrostatic pressure of natural contaminating microorganisms and inoculated salmonella typhimurium and E. Coli O157:H7 on insect protein-based gel particles. *LWT, 133*, Article 109948. https://doi.org/10.1016/J.LWT.2020.109948

Mohd Fauziee, N. A., Chang, L. S., Wan Mustapha, W. A., Md Nor, A. R., & Lim, S. J. (2021). Functional polysaccharides of fucoidan, laminaran and alginate from malaysian brown seaweeds (Sargassum polycystum, Turbinaria ornata and Padina boryana). *International Journal of Biological Macromolecules, 167*, 1135–1145. https://doi.org/10.1016/j.ijbiomac.2020.11.067

Montes, L., Gisbert, M., Hinojosa, I., Sineiro, J., & Moreira, R. (2021). Impact of drying on the sodium alginate obtained after polyphenols ultrasound-assisted extraction from Ascophyllum nodosum seaweeds. *Carbohydrate Polymers, 272*, Article 118455. https://doi.org/10.1016/J.CARBPOL.2021.118455

Mørch, Ý. A., Donati, I., Strand, B. L., & Skjåk-Bræk, G. (2006). Effect of Ca2+, Ba2+, and Sr2+ on alginate microbeads. *Biomacromolecules, 7*(5), 1471–1480. https://doi.org/10.1021/BM060010D/ASSET/IMAGES/LARGE/BM-2006-00010D_0009.JPEG

Navarro-López, E., López-Rodríguez, M., Acién-Fernández, F. G., Molina-Grima, E., & Cerón-García, M.d. C. (2020). Biostimulants obtained after pilot-scale high-pressure homogenization of Scenedesmus sp. grown in pig manure. *Algal Research, 52*, 102123. https://doi.org/10.1016/J.ALGAL.2020.102123

Okolie, C. L., Mason, B., Mohan, A., Pitts, N., & Udenigwe, C. C. (2020). Extraction technology impacts on the structure-function relationship between sodium alginate extracts and their in vitro prebiotic activity. *Food Bioscience, 37*, Article 100672. https://doi.org/10.1016/j.fbio.2020.100672

Parthiban, C., Parameswari, K., Saranya, C., Hemalatha, A., & Anantharaman, P. (2012). Production of sodium alginate from selected seaweeds and their physiochemical and biochemical properties. *Asian Pacific Journal of Tropical Biomedicine, 1*, 1–4.

Pinton, M. B., dos Santos, B. A., Lorenzo, J. M., Cichoski, A. J., Boeira, C. P., & Campagnol, P. C. B. (2021). Green technologies as a strategy to reduce NaCl and phosphate in meat products: An overview. *Current Opinion in Food Science, 40*, 1–5. https://doi.org/10.1016/J.COFS.2020.03.011

Rastogi, N. K., Raghavarao, K. S. M. S., Balasubramaniam, V. M., Niranjan, K., & Knorr, D. (2010). In *, 47. Opportunities and Challenges in High Pressure Processing of Foods* (pp. 69–112). https://doi.org/10.1080/10408390600626420 (1).

Re, R., Pellegrini, N., Proteggente, A., Pannala, A., Yang, M., & Rice-Evans, C. (1999). Antioxidant activity applying an improved ABTS radical cation decolorization assay. *Free Radical Biology and Medicine, 26*(9–10), 1231–1237. https://doi.org/10.1016/S0891-5849(98)00315-3

Rinaudo, M. (2007). Seaweed polysaccharides. Elsevier *Comprehensive Glycoscience, 2*(2), 691–735 https://hal.archives-ouvertes.fr/hal-00305758.

Sanjeewa, K. K. A., Kang, N., Ahn, G., Jee, Y., Kim, Y.-T., & Jeon, Y.-J. (2018). Bioactive potentials of sulfated polysaccharides isolated from brown seaweed sargassum spp in related to human health applications: A review. *Food Hydrocolloids, 81*, 200–208. https://doi.org/10.1016/J.FOODHYD.2018.02.040

Saravana, P. S., Cho, Y.-N., Woo, H.-C., & Chun, B.-S. (2018). Green and efficient extraction of polysaccharides from brown seaweed by adding deep eutectic solvent in subcritical water hydrolysis. *Journal of Cleaner Production, 198*, 1474–1484. https://doi.org/10.1016/J.JCLEPRO.2018.07.151

Schultz, S., Wagner, G., Urban, K., & Ulrich, J. (2004). High-pressure homogenization as a process for emulsion formation. *Chemical Engineering & Technology, 27*(4), 361–368. https://doi.org/10.1002/CEAT.200406111

Sellimi, S., Younes, I., Maalej, H., Montero, V., Rinaudo, M., Dahia, M., Mechichi, T., Hajji, M., Nasri, M., & ben Ayed, H. (2015). Structural, physicochemical and antioxidant properties of sodium alginate isolated from a Tunisian brown seaweed. *International Journal of Biological Macromolecules, 72*, 1358–1367. https://doi.org/10.1016/j.ijbiomac.2014.10.016

Singleton, V. L., Orthofer, R., & Lamuela-Raventós, R. M. (1999). Analysis of total phenols and other oxidation substrates and antioxidants by means of Folin-Ciocalteu reagent. *Methods in Enzymology, 299*, 152–178. https://doi.org/10.1016/S0076-6879(99)99017-1

Siriwardhana, N., Kim, K. N., Lee, K. W., Kim, S. H., Ha, J. H., Song, C. B., Lee, J. B., & Jeon, Y. J. (2008). Optimisation of hydrophilic antioxidant extraction from hizikiafusiformis by integrating treatments of enzymes, heat and pH control. *International Journal of Food Science & Technology, 43*(4), 587–596. https://doi.org/10.1111/J.1365-2621.2006.01485.X

Suwal, S., Perreault, V., Marciniak, A., Tamigneaux, É., Deslandes, É., Bazinet, L., Jacques, H., Beaulieu, L., & Doyen, A. (2019). Effects of high hydrostatic pressure and polysaccharidases on the extraction of antioxidant compounds from red macroalgae, Palmaria palmata and Solieria chordalis. *Journal of Food Engineering, 252*, 53–59. https://doi.org/10.1016/J.JFOODENG.2019.02.014

Ummat, V., Sivagnanam, S. P., Rajauria, G., O'Donnell, C., & Tiwari, B. K. (2021). Advances in pre-treatment techniques and green extraction technologies for bioactives from seaweeds. *Trends in Food Science & Technology, 110*, 90–106. https://doi.org/10.1016/J.TIFS.2021.01.018

Wiles, P. G., Gray, I. K., Kissling, R. C., Delahanty, C., Evers, J., Greenwood, K., Grimshaw, K., Hibbert, M., Kelly, K., Luckin, H., McGregor, K., Morris, A.,

Petersen, M., Ross, F., Valli, M., & Valli, M. (1998). Routine analysis of proteins by Kjeldahl and Dumas methods: Review and interlaboratory study using dairy products. *Journal of AOAC International, 81*(3), 620–632. https://doi.org/10.1093/jaoac/81.3.620

Yang, M., Zhou, D., Xiao, H., Fu, X., Kong, Q., Zhu, C., Han, Z., & Mou, H. (2022). Marine-derived uronic acid-containing polysaccharides: Structures, sources, production, and nutritional functions. *Trends in Food Science & Technology, 122*, 1–12. https://doi.org/10.1016/J.TIFS.2022.02.013

Zhao, S., Baik, O. D., Choi, Y. J., & Kim, S. M. (2014). In *, 54. Pretreatments for the Efficient Extraction of Bioactive Compounds from Plant-Based Biomaterials* (pp. 1283–1297). https://doi.org/10.1080/10408398.2011.632698 (10).

Zhao, X., Li, B., Xue, C., & Sun, L. (2012). Effect of molecular weight on the antioxidant property of low molecular weight alginate from Laminaria japonica. *Journal of Applied Phycology, 24*(2), 295–300. https://doi.org/10.1007/S10811-011-9679-Y/FIGURES/4

Zrid, R., Bentiss, F., Attoumane Ben Ali, R., Belattmania, Z., Zarrouk, A., Elatouani, S., Eddaoui, A., Reani, A., & Sabour, B. (2016). Potential uses of the brown seaweed Cystoseira humilis biomass: 1- Sodium alginate yield, FT-IR, 1H NMR and rheological analyses. *Journal of Materials and Environmental Science, 7*(2), 613–620.

Zuluaga, C., Martínez, A., Fernández, J., López-Baldó, J., Quiles, A., & Rodrigo, D. (2016). Effect of high pressure processing on carotenoid and phenolic compounds, antioxidant capacity, and microbial counts of bee-pollen paste and bee-pollen-based beverage. *Innovative Food Science & Emerging Technologies, 37*, 10–17. https://doi.org/10.1016/J.IFSET.2016.07.023